The 2016 World Congress on
Advances in Civil, Environmental, and Materials Research (ACEM16)
Jeju Island, Korea, August 28-September 1, 2016

Tornado-induced effects on aerostatic and aeroelastic behaviors of long-span bridge

Jianming Hao[1)] and *Teng Wu[2)]

[1), 2)] *Department of Civil, Structural and Environmental Engineering, University at Buffalo, Buffalo, NY 14206, USA*

ABSTRACT

This study focuses on the tornado-induced effects on long-span bridge that is extremely sensitive to winds. Specifically, the non-uniformity, transient and intensive vertical wind velocity natures of tornado event and their effects on the flexible long-span bridge are investigated. The nonlinear aerostatic analysis approach based on the finite element model and the time-domain aeroelastic stability analysis method based on the 2-D indicial response function are utilized in this study. The aerostatic and aeroealstic behaviors of bridge under tornado event are compared with those subject to equivalent synoptic wind event. The results from this study could be used to highlight the effects due to abovementioned tornado natures, and facilitate more appropriate design of flexible long-span bridge considering non-synoptic wind loads.

1. INTRODUCTION

The tornado is known as one type of non-synoptic wind events that has violent impacts and frequent occurrence on the earth's surface. The high wind velocity and significant pressure change due to the tornados could result in serious damage or collapse of structures. Compared with vertical structures like residential buildings, the line-like horizontal structures such as the long-span bridges have a higher probability to meet the tornadoes (Tamura, 2009). For example, the Kinzua Bridge in the U.S. state of Pennsylvania was struck by tornado in 2003 and large portion of the bridge collapsed. In addition, long-span bridges are more likely to be built in coastline area, which are prone to suffering the tornado events produced by typhoon/hurricane. Thus, it is important to investigate the performance of the long-span bridge subject to tornado winds.

The wind velocity profile of tornado is characterized as transient in time and horizontally non-uniform in space, together with intensive vertical wind flow. These features may significantly change bridge aerodynamics. In this study, the nonlinear aerostatic analysis approach based on the finite element model and aeroelastic stability

[1)] Graduate Student
[2)] Assistant Professor, mail: [2)] tengwu@buffalo.edu

analysis method based on the 2-D indicial response function in time domain are utilized to exam aerostatic and aeroelastic behaviors subject to tornado event, respectively. By comparing with the behaviors under equivalent synoptic wind events, the results could be used to highlight the effects due to tornado natures, and facilitate more appropriate design of flexible long-span bridge considering non-synoptic wind loads.

2. THEORETICAL BACKGROUND

Nonlinear aerostatic analysis framework based on quasi-stead model is utilized herein to investigate the effects due to the non-uniform and transient features of tornado event on long-span bridge performance. In order to consider the intensive vertical wind effect, the lift force induced by vertical wind could be added to this model. On the other hand, the semi-empirical linear model in time domain is applied to simulate the aeroelastic forces, where the 2-D indicial response function proposed by Hao and Wu (2016) is employed here to represent the bridge aerodynamics induced by transient effects. The theoretical background of these analysis frameworks will be discussed in the following of this section.

2.1 Aerostatic analysis

The quasi-steady (QS) model was used by Zhang et al. (2010) for investigating the turbulence effect on aerostatic instability and recently Chen (2014) to consider the time-varying mean wind velocity effects on aerodynamic forces. Similarly, the QS theory-based model could be utilized to characterize the tornado induced wind loads acting on the bridge deck, where the static nonlinear relationship between the incident flow and the flow-induced forces on bridge at each time instant could be described. **Figure 1** shows the coordinate for aerostatic forces on the unit-span bridge deck section.

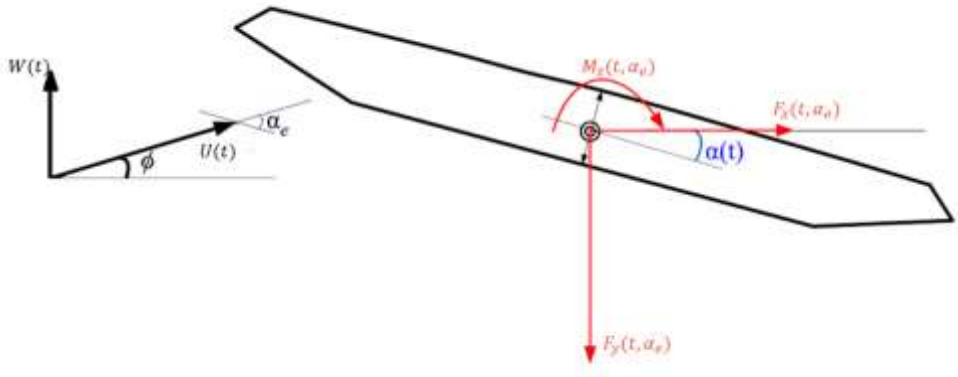

Figure 1. Coordinate for aerostatic forces acting on bridge deck section

The drag force, lift force and torsional moment per unit-span in global bridge coordinates under tornado wind are expressed as

$$F_y(t,\alpha_e) = F_L(t,\alpha_e)\cos(\phi) - F_D(t,\alpha_e)\sin(\phi) - F_W(t,\alpha_{ew}), \quad (1)$$

$$F_x(t,\alpha_e) = F_L(t,\alpha_e)\sin(\phi) + F_D(t,\alpha_e)\cos(\phi), \quad (2)$$

$$M_z(t,\alpha_e) = M(t,\alpha_e), \quad (3)$$

where

$$F_L(t,\alpha_e) = -\frac{1}{2}\rho U(t)^2 B C_L(\alpha_e), \quad (4)$$

$$F_D(t,\alpha_e) = \frac{1}{2}\rho U(t)^2 B C_D(\alpha_e) + \frac{\pi}{4}\rho C_{IN} D^2 \frac{dU(t)}{dt}, \quad (5)$$

$$F_W(t,\alpha_e) = \frac{1}{2}\rho W(t)^2 B C_W(\alpha_{ew}), \quad (6)$$

$$M(t,\alpha_e) = \frac{1}{2}\rho U(t)^2 B^2 C_M(\alpha_e) \quad (7)$$

where ρ is the air density; B is the bridge deck width; C_L, C_D and C_M are non-dimensional steady-state coefficients which could be obtained experimentally; C_W is the aerostatic coefficients of the bridge deck under vertical wind flow, which are obtained numerically; α_e is the effective angle of attack which is the summation of the torsional displacement of the bridge deck at each time instant denoted by "$\alpha(t)$" and initial angle of attack denoted by "ϕ", while α_{ew} is the effective angle of attack subject to vertical wind flow and equal to $90 - \alpha_e + \phi$; $U(t)$ and $W(t)$ are the oncoming mean wind velocity of tornado event in horizontal and vertical direction, respectively, both of which vary with time. It should be noted that, due to the nature of tornado event, the inertial force of tornado cannot be neglected (Wen and Chu, 1973). Actually, the second term of the F_D represents the inertial force caused by tornado wind and C_{IN} is the inertial coefficients which can be determined as 1.3 according to the study by Sarpkaya and Garrison (1963).

Based on the QS model, the analysis procedure is developed to investigate the aerostatic behavior of bridge subject to tornado wind event. The general steps of this procedure can be expressed as follow,

1) Develop the finite element model of the bridge in the commercial software;
2) Simulate the tornado wind profile time history at each node along the bridge span;
3) Calculate the wind loads on each nodes at the initial time with initial angle of attack and wind speed;
4) Solve the nonlinear static problem to obtain the displacements of bridge deck at the current time instant;
5) Calculate the effective angle of attack α_e based on the initial angle of attack ϕ

and current time torsional displacement of bridge deck $\alpha(t)$, which will be used as the effective angle of attack to calculate the wind loads for the next time instant;

6) Repeat the step 4 and step 5 until the end of the simulated tornado wind profile time history.

2.2 Aeroelastic analysis

The time-domain aeroealstic lift force and torsional moment of bridge deck using the aeroelastic unit-step response function can be expressed as

$$L_{ae}(s)=\frac{1}{2}\rho U^2 B C_L^{'}\left[\left\{\varphi_{L\alpha}(s)\alpha(0)+\int_0^s \varphi_{L\alpha}(s-\sigma)\alpha^{'}(\sigma)d\sigma\right\}+\left\{\varphi_{Lh}(s)\frac{h^{'}(0)}{B}+\int_0^t \varphi_{Lh}(s-\sigma)\frac{h^{''}(\sigma)}{B}d\sigma\right\}\right] \tag{8}$$

$$M_{ae}(s)=\frac{1}{2}\rho U^2 B^2 C_M^{'}\left[\left\{\varphi_{M\alpha}(s)\alpha(0)+\int_0^s \varphi_{M\alpha}(s-\sigma)\alpha^{'}(\sigma)d\sigma\right\}+\left\{\varphi_{Mh}(s)\frac{h^{'}(0)}{B}+\int_0^s \varphi_{Mh}(s-\sigma)\frac{h^{''}(\sigma)}{B}d\sigma\right\}\right] \tag{9}$$

where $s=Ut/B$ is the dimensionless time; the prime indicates derivative with respect to non-dimensional time. $\varphi(s)$ represents the aeroealstic unit-step response function, which can be approximately expressed as (Scanlan et al., 1974),

$$\varphi_{yx}(s)=1-\sum_{i=1}^{n} a_{iyx}e^{-b_{iyx}s} \tag{10}$$

where *y* is the lift force *L* or torsional moment *M*; *x* is the input motion *h* or α; and *n* is determined from the aerodynamic properties of the bridge deck. Parameters *"a"* and *"b"* are constant coefficients which can be identified by the "semi-inverse" approach (Scanlan et al., 1974). The physical meaning of the dimensionless time, denoted as *"s"*, is the convected distance of the wake in terms of the chord length *"B"*. Apparently, the convected distance of wake is depended on the flow velocity and wake convected time. Substituting $s=Ut/B$ into Eq.(10), the aeroelastic unit-step response function with respect to the physical time could be expressed as

$$\varphi_{yx}(t)=1-\sum_{i=1}^{n} a_{iyx}e^{-b_{iyx}\frac{U}{b}t} \tag{11}$$

As the mean wind velocity of the tornado event varies with time, an additional time scale should be considered in the abovementioned indicial response function to represent the characteristics of the bridge aerodynamics subject to the transient effects. As a result, the enhanced aeroelastic unit-step response function could be expressed as

$$\varphi_{yx}\left(t;U(\tau)\right)=1-\sum_{i=1}^{n}a_{iyx}e^{-b_{iyx}\frac{U(\tau)}{B}t} \tag{12}$$

In this formulation, "τ" represents a time scale in the change of wind-structure interaction system, i.e. change of mean wind speed, while "*t*" indicates a time scale in the convection of the flow wake. **Figure 2** illustratively shows an example to evaluate the aeroelastic system response under non-synoptic winds with a time-varying mean wind speed at physical time t=2.

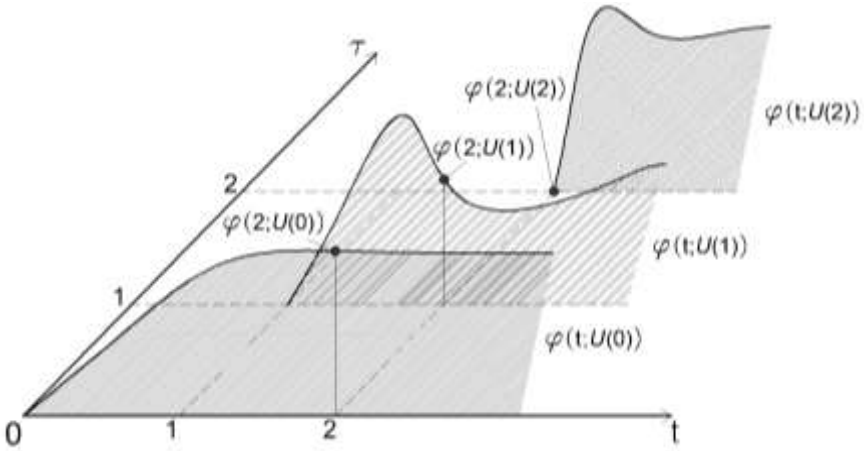

Figure 2. Schematic of a typical 2-D unit-step response function

Consequently, the aeroelastic force (or moment) of bridge deck subject to the tornado winds can be determined as

$$\begin{aligned}L_{ae}\left(t\right)=\frac{1}{2}\rho U(t)^2BC_L^{'}\Bigg[&\left\{\varphi_{L\alpha}\left(t;U(0)\right)\alpha\left(0\right)+\int_0^t\varphi_{L\alpha}\left(t-\sigma;U(\sigma)\right)\dot{\alpha}\left(\sigma\right)d\sigma\right\}\\&+\left\{\varphi_{Lh}\left(t;U(0)\right)\frac{\dot{h}(0)}{B}+\int_0^t\varphi_{Lh}\left(t-\sigma;U(\sigma)\right)\frac{\ddot{h}(\sigma)}{B}d\sigma\right\}\Bigg]\end{aligned} \tag{13}$$

$$\begin{aligned}M_{ae}\left(t\right)=\frac{1}{2}\rho U(t)^2B^2C_L^{'}\Bigg[&\left\{\varphi_{M\alpha}\left(t;U(0)\right)\alpha\left(0\right)+\int_0^t\varphi_{M\alpha}\left(t-\sigma;U(\sigma)\right)\dot{\alpha}\left(\sigma\right)d\sigma\right\}\\&+\left\{\varphi_{Mh}\left(t;U(0)\right)\frac{\dot{h}(0)}{B}+\int_0^t\varphi_{Mh}\left(t-\sigma;U(\sigma)\right)\frac{\ddot{h}(\sigma)}{B}d\sigma\right\}\Bigg]\end{aligned} \tag{14}$$

3. MODELING OF TORNADO WIND FIELD AND BRIDGE

In this study, the time-varying mean wind velocity of the tornado at different bridge spanwise locations are simulated by utilizing the empirical models introduced by earlier researchers to highlight the transient and non-uniform features, while the turbulence is neglected due the high wind speed and short duration of tornado impact on long-span bridge.

3.1 Modeling of tornado field

The tornado model employed in this study is based on the theoretical model of the three-dimensional flow in the boundary layer of a tornado-like vortex presented by Kuo (1971). The corresponding mathematical model was developed by Wen and Chu (1973), where the wind velocity profiles within and above the boundary layer are different and described separately. The boundary layer thickness is very small at the center of the core and then increases rapidly with radial distance, and eventually achieves a relatively large and constant value. In this study, the selected F3 tornado has the maximum tangential velocity above the boundary layer of 92 m/s, the radial distance from the center where the tangential velocity above the boundary layer is a maximum of 60.9 m and a translational velocity of 20 m/s. The thickness of the boundary layer far from the tornado core is 600 m. The thickness of the boundary layer near the core follows the relation with radial distance shown as

$$\delta(r') = \delta_0\left[1-\exp\left(-0.5r^2\right)\right] \tag{15}$$

where r' is the radial distance; $r = r'/r_{max}$, r_{max} is the radial distance from the center where the tangential velocity above the boundary layer is a maximum; and δ_0 is the thickness where $r \gg 1$. The elevation of bridge is 69.3 m. The start location of the tornado is set as 2 km upwind of the structure location, and with a duration of 140 s. Since the tornado events are localized and have a comparative or even smaller size compared to the long-span bridges, various tornado wind paths relative to the bridge location are examined. A sketch of the wind path related to the structure is presented in **Figure 3**. In the figure, "*o*" is the center of the tornado, r_{max} is the radius of maximum tangential wind velocity. The path of the tornado center shown in the figure indicates the most unfavorable loading condition of the structure.

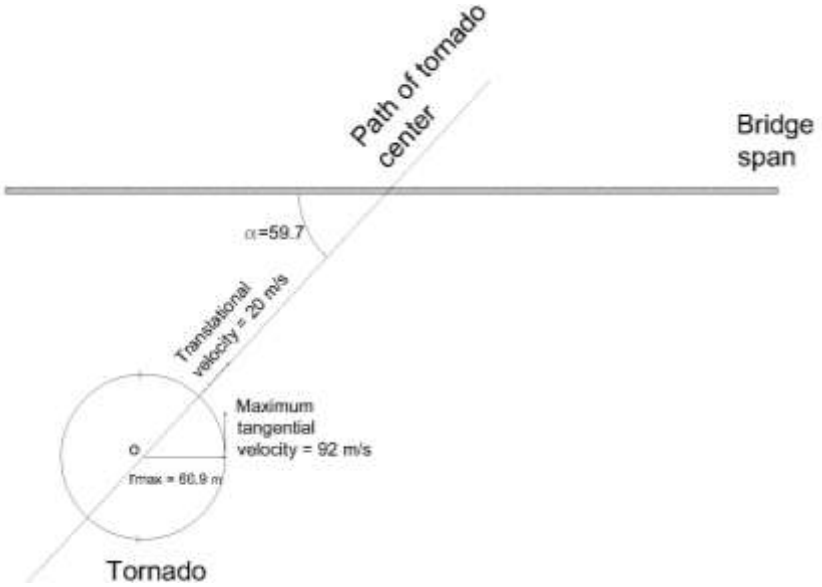

Figure 3. Sketch of the tornado related to structure

Figures 4(a) and 4(b) show the horizontal and vertical time-varying mean wind velocity at the midspan locations, respectively. **Figures 4(c)** represents the horizontal distribution of the wind profile along span at a specific time instant. Similarly, the time-varying mean wind velocity of tornado at each location along span could also be generated. Accordingly, this model is sufficient for illustrating the transient and non-uniform features of tornado. It should be noted that the averaged value of the time-varying mean wind speed of the tornado over the total simulation duration is identical to translational speed 20 m/s. Hence, the constant mean wind speed of the equivalent synoptic case could be set as 20 m/s for a meaningful comparison. Since the selected path of tornado in this study is not perpendicular to the bridge span, the beginning wind velocity at the midspan location is not equal to 20 m/s.

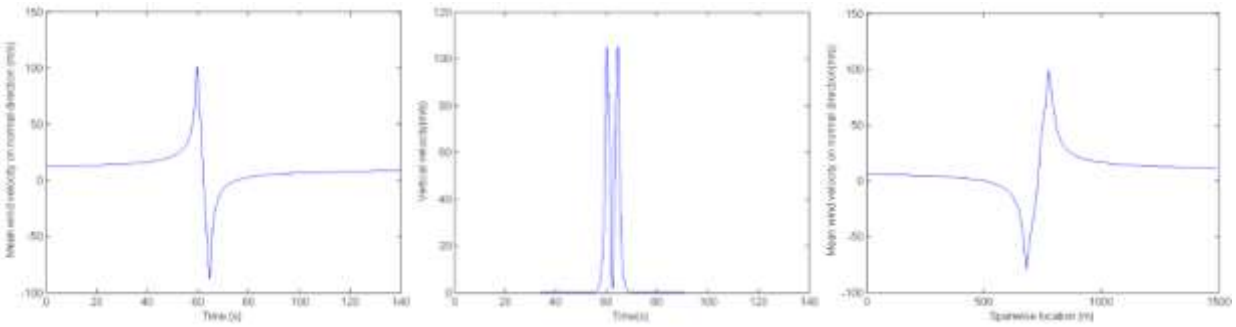

Figure 4. Tornado wind profile: a) ,b) Time-varying mean wind velocity at midspan location in horizontal direction and vertical direction; c) Horizontal distribution of *U(t)* along span at time = 68.1 *s*.

3.2 Modeling of long-span bridge

For the modeling of structure, the long span bridge finite element (FE) model is developed based on spine beam model with equivalent sectional properties. The geometric non-linearity could be considered in this model and it has good accuracy to

exam the global behaviors of bridge subject to aerostatic and aeroelastic loads. In order to effectively investigate the behavior of structures due to the horizontal non-uniformity of winds, accurately modelling of wind force distribution on the finite element model is important. Unlike the conventional mesh method for the suspension bridge, where the mesh size is usually selected as the interval length between hangers, the mesh size in this study depends on the discretization of the wind field along the spanwise, which is typically smaller than the conventional mesh size for accurately describing the non-uniform feature of tornado wind.

4. NUMERICAL EXAMPLES AND DISCUSSIONS

In this study, a long-span suspension bridge with 1490m main span is chosen as a numerical example. The FE model developed in commercial software and the geometric configuration of the bridge deck cross section are depicted in **Figure 5**.

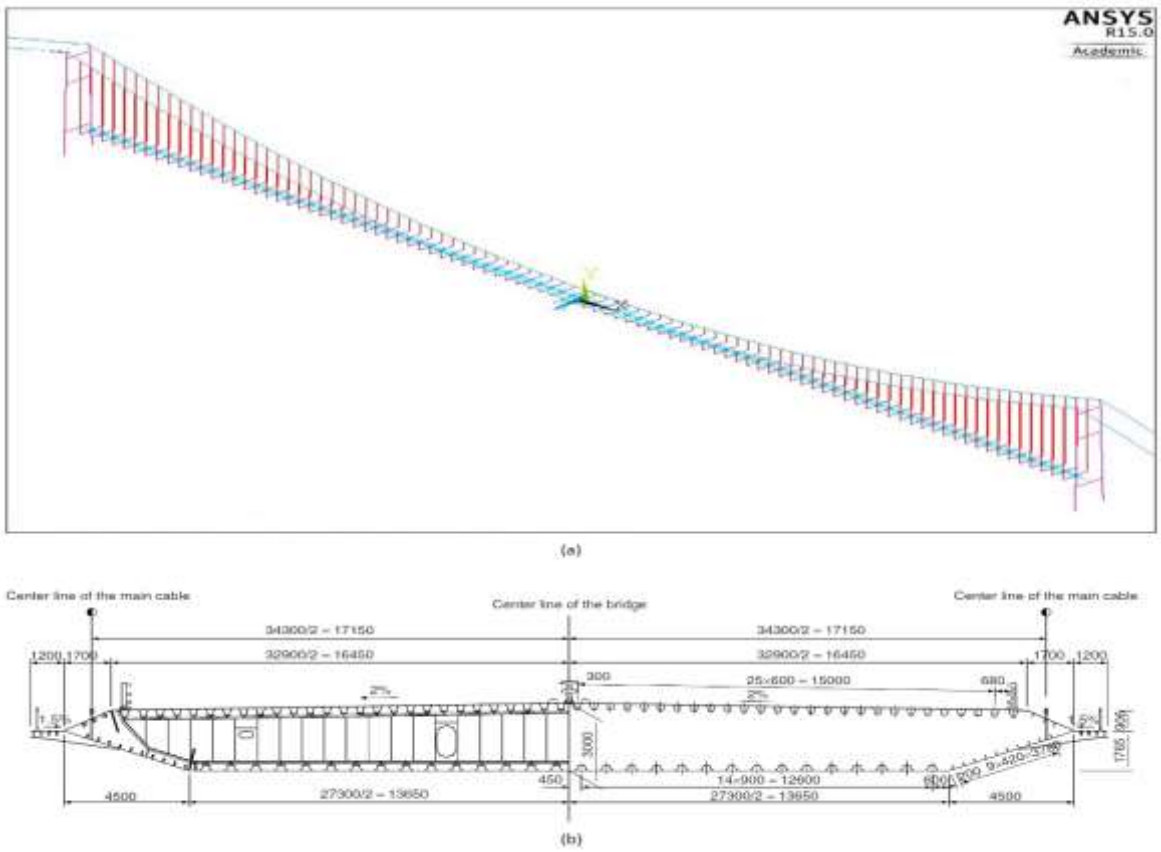

Figure 5. a) FE model; b) bridge deck cross section (Wang et al., 2010)

The width of the example bridge deck section is 38.7 m; the mass per unit length is 21686 kg; and the mass moment inertial per unit length is 2820000 kg.m^2. The natural frequency of first vertical and first torsional modes are 0.0879 and 0.2284 Hz, respectively. The damping ratios are set as 0.5% for both modes. Both the aerostatic and aeroelastic analysis are based on this engineering background.

4.1 Aerostatic analysis

In this analysis, the 3-D FE model of the bridge was established in commercial software to investigate the non-uniform and transient effects on the aerostatic behavior of the bridge. The main span was discretized into 184 beam elements which could well model the non-uniform wind distribution along the span. This FE model has been validated by comparing its modal properties with the results from other researcher's report. The natural frequencies and mode shapes of first 20 modes show good agreement with the study by Chen et al. (2002).

Figure 6 shows the aerostatic coefficients of bridge deck, where the C_L, C_D and C_M are measured experimentally in the wind tunnel tests (Chen et al., 2002) and C_W are obtained by CFD simulation. By comparing with the steady state coefficients of a flat plate under 90^o (Taira et al., 2007), the CFD simulations show good agreement with the order of the magnitude of the experimental results. This indicates the CFD results have good fidelity for the aeroestatic analysis in this study.

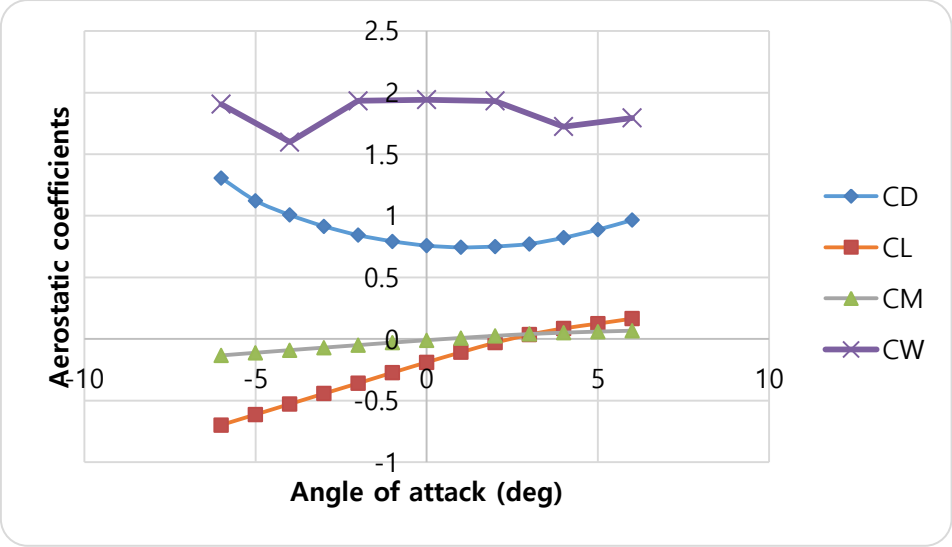

Figure 6. Aerostatic coefficients of bridge deck

Based on the FE model and aerostatic parameters of this example bridge, the aerostatic analysis could be processed following the procedures illustrated in section 2.1. The comparison of the maximum values of bridge deck vertical displacements at various spanwise locations between the tornado case and the equivalent synoptic case are plotted in **Figure 7**. **Figure 8** displays the comparison of the time history of the bridge deck vertical displacements at center of main span between this two cases. It can be noted from these results that, the tornado effects on the long-span bridge aerostatic behavior show intensively localized feature with relatively short duration. In addition, the vertical displacements under the tornado event have larger magnitude compared with synoptic wind case. This is mainly due to the intensive vertical wind velocity.

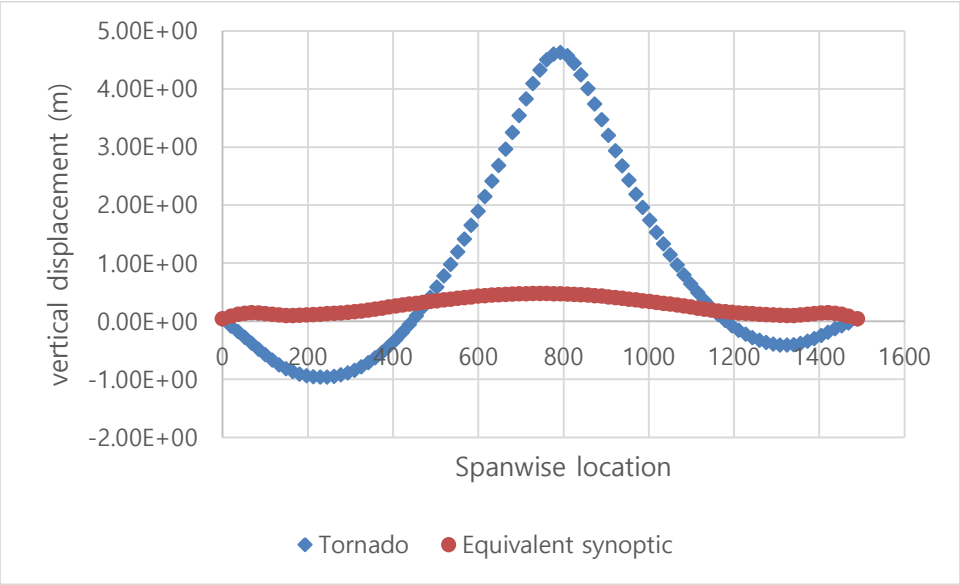

Figure 7. Comparison of maximum values of bridge deck vertical displacements at various spanwise locations at time=68.1 *s*

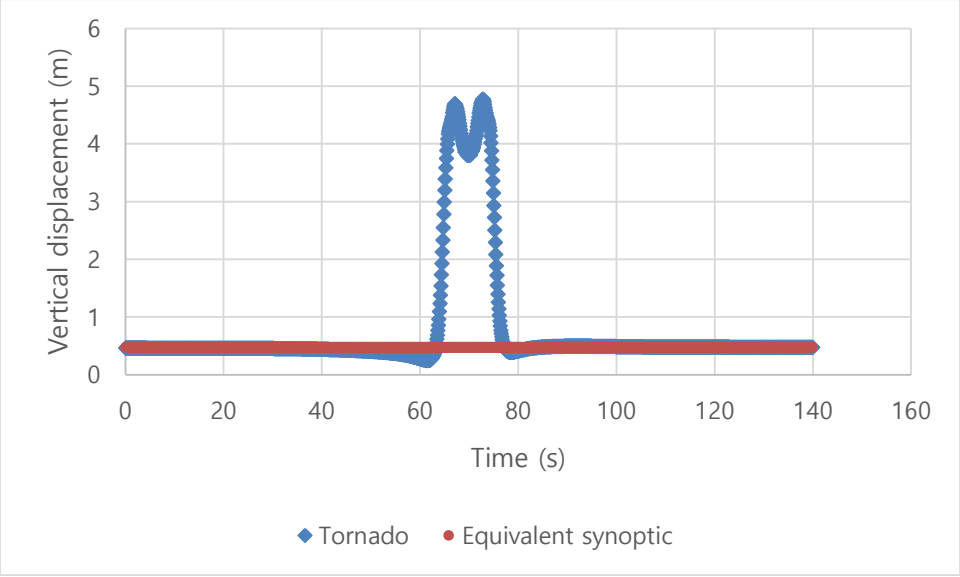

Figure 8. Comparison of the bridge deck vertical displacements time history at center of main span

4.2 Aeroelastic analysis

A unit-length of bridge deck section is utilized to investigate the effects of the transient feature of tornado event on the aeroelastic instability. Base on the flutter derivatives of this example bridge deck experimentally measured in the wind tunnel (Chen et al., 2002), the aeroelastic unit-step response function can be identified using the “semi-inverse” approach (Scanlan et al., 1974). According to the framework illustrated in section 2.2, the 2-D indicial response functions under the tornado event with a time-varying mean wind speed can be extended from the 1-D cases. The four

fundamental 2-D aeroelastic indicial response functions are plotted in **Figure 9**. The bridge response is then calculated using the step-by-step time integration method.

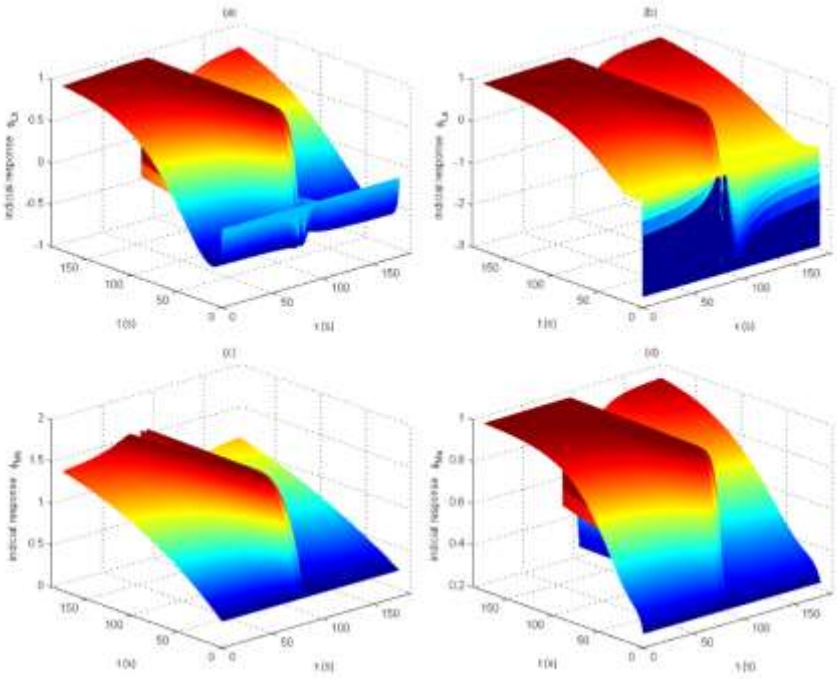

Figure 9. 2-D aeroelastic indicial response function under tornado wind

The investigation of the aeroelastic instability under synoptic wind event was conducted firstly. It should be noted that, the 1-D indicial response function where the bridge is subject to the synoptic wind event with a constant mean wind speed for all τ is a special case of the 2-D indicial response function. The time history of the vertical and torsional motion-induced responses under the onset flutter critical velocity *Ucr = 57.2 m/s* are depicted in **Figure 10**, which shows good agreement with the wind tunnel test result as *Ucr = 58.1 m/s.* This indicates that the employed analysis approach has good fidelity for non-synoptic aeroelastic analysis.

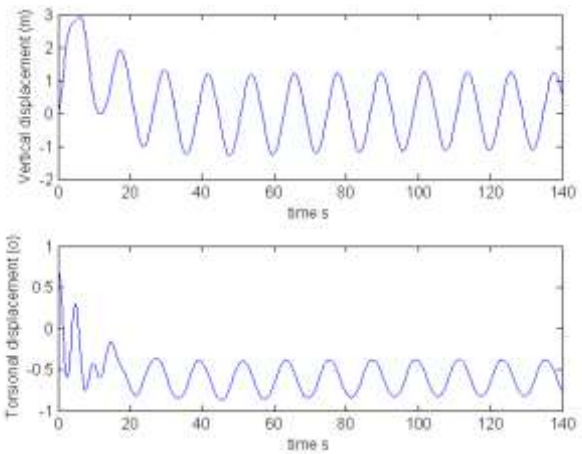

Figure 10. Motion-induced responses at flutter critical speed

Figure 11 shows the calculated motion-induced responses based on the current analysis framework subject to the tornado wind event. As shown in the figure, as the mean wind speed approaches to a high magnitude, the response will increase abruptly to a large value, but will not diverge. The phenomenon indicates that, although the instantaneous wind speed is larger than the critical flutter wind speed, the aeroelastic instability cannot occur under tornado wind event which presents transient feature. This mainly attributes to the lack of the build-up time for structure to sustain a high level of response. The build-up time decreases with the increase of the the structure damping ratio and frequency (Chen, 2014). In other words, the long-span bridges, which have lower frequency and damping ratio, have longer build-up time for the aeroelastic instability. Therefore, it is necessary that the extreme wind events have enough long duration to initiate the aeroelastic instability of the long-span bridge.

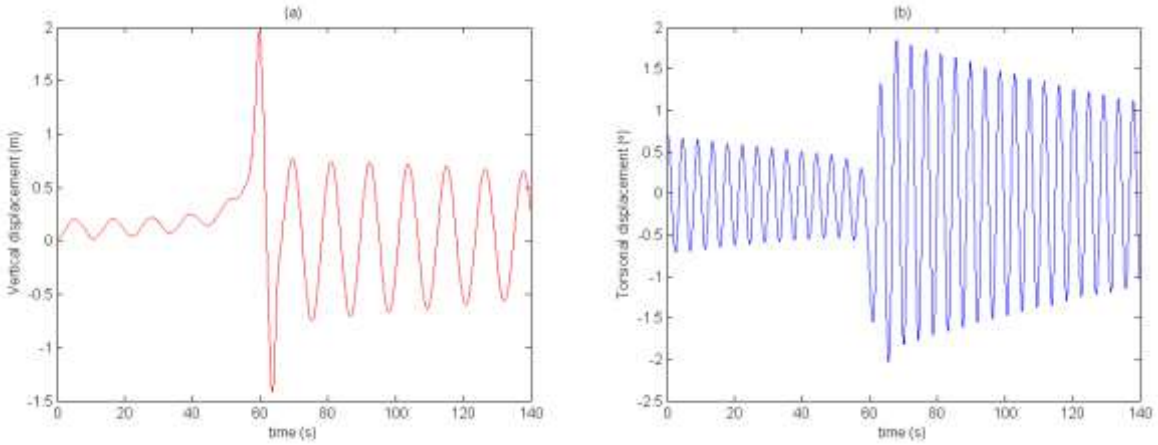

Figure 11. Motion-induced responses using 2-D indicial response function under tornado wind event

5. CONCLUDING REMARKS

The nonlinear aerostatic analysis based on the quasi-steady model and aeroelastic analysis based on the 2-D indicial response function are presented in this study to highlight the effects of transient nature, non-uniformity and intensive vertical wind velocity under tornado winds. The refined finite element model is used to model the structure for better capturing the non-uniform effects. CFD simulation is conduct to account for the significant vertical wind effects on bluff-body aerodynamics. A typical long-span suspension bridge is utilized as a numerical example to emphasize the tornado induced effects on structure performance. The results based on the numerical examples show that: 1) the non-uniform and localized nature has intensive impact on the long-span structure; 2) due to the intensive vertical wind velocity, the vertical displacement is significant larger compared to the equivalent synoptic wind event; 3) the transient nature could significantly modify the bridge aerodynamics which can be represented by the 2-D indicial response function; and 4) there is no aeroelastic instability occurred under tornado wind event which may be due to the lack of the build-up time for the structure. The relation between the extreme wind impact duration on the structure and the build-up time is an interesting topic that need to be investigated in the future study.

REFERENCES

Chen, 2014. Analysis of multimode coupled buffeting response of long-span bridges to nonstationary winds with force parameters from stationary wind. Journal of Structural Engineering 141, 04014131.

Chen, Guo, Z., Zhou, Z., Ma, R. and Wang, D., 2002. Study of Aerodynamic Performance of Runyang Bridge. Technical Report WT200218.

Hao, J. and Wu, T., 2016. Non-synoptic wind-induced effects on linear bluff-body aerodynamics. Proceedings of 8th International Colloquium on Bluff-Body Aerodynamics and its Application (BBAAVIII), Boston.

Kuo, H., 1971. Axisymmetric flows in the boundary layer of a maintained vortex. Journal of the Atmospheric sciences 28, 20-41.

Sarpkaya, T. and Garrison, C., 1963. Vortex formation and resistance in unsteady flow. Journal of Applied Mechanics 30, 16-24.

Scanlan, R., Budlong, K. and Béliveau, J., 1974. Indicial aerodynamic functions for bridge decks. Journal of Sanitary Engineering Division 100.

Taira, K., Dickson, W.B., Colonius, T., Dickinson, M.H. and Rowley, C.W., 2007. Unsteadiness in flow over a flat plate at angle-of-attack at low Reynolds numbers. AIAA Paper 710, 2007.

Tamura, Y., 2009. Wind induced damage to buildings and disaster risk reduction. Proceedings of the APCWE-VII, Taipei, Taiwan.

Wang, H., Li, A., Hu, R. and Li, J., 2010. Accurate stress analysis on steel box girder of long span suspension bridges based on multi-scale submodeling method. Advances in Structural Engineering 13, 727-740.

Wen, Y.-K. and Chu, S.-L., 1973. Tornado risks and design wind speed. Journal of the Structural Division 99, 2409-2421.

Zhang, Z., Chen, Z., Hua, X., Li, C. and Ge, Y.J., 2010. Investigation of turbulence effects on torsional divergence of long-span bridges by using dynamic finite-element method. Journal of Bridge Engineering 15, 639-652.